Published OnlineFirst January 31, 2007; DOI: 10.1158/1535-7163.MCT-06-0468

Inhibition of fibroblast to myofibroblast transition by halofuginone contributes to the chemotherapy-mediated antitumoral effect

Yuval Sheffer,[1] Oded Leon,[1] Jehonathan H. Pinthus,[2] Arnon Nagler,[3] Yoram Mor,[4] Olga Genin,[1] Maya Iluz,[1] Norifumi Kawada,[5] Katsutoshi Yoshizato,[6] and Mark Pines[1]

[1]Institute of Animal Science, Agricultural Research Organization, Volcani Center, Bet Dagan, Israel; [2]Department of Surgery, McMaster University, Hamilton, Ontario, Canada; [3]Division of Hematology and [4]Department of Urology, Chaim Sheba Medical Center, Tel Hashomer, Israel; [5]Department of Hepatology, Graduate School of Medicine, Osaka City University, Osaka, Japan; and [6]Developmental Biology Laboratory, CLUSTER Project, and 21st Century COE Program, Department of Biological Science, Graduate School of Science, Hiroshima University, Higashi-Hiroshima, Japan

Abstract

Stromal myofibroblasts play an important role in tumor progression. The transition of fibroblasts to myofibroblasts is characterized by expression of smooth muscle genes and profuse synthesis of extracellular matrix proteins. We evaluated the efficacy of targeting fibroblast-to-myofibroblast transition with halofuginone on tumor progression in prostate cancer and Wilms' tumor xenografts. In both xenografts, low doses of halofuginone treatment, independent of the route of administration, resulted in a trend toward inhibition in tumor development. Moreover, halofuginone synergizes with low dose of docetaxel in prostate cancer and vincristine and dactinomycin in Wilms' tumor xenografts, resulting in significant reduction in tumor volume and weight comparable to the effect observed by high doses of the respective chemotherapies. In prostate cancer and Wilms' tumor xenografts, halofuginone, but not the respective chemotherapies, inhibited the synthesis of collagen type I, α-smooth muscle actin, transgelin, and cytoglobin, all of which are characteristics of activated myofibroblasts. Halofuginone, as the respective chemotherapies, increased the synthesis of Wilms' tumor suppressor gene product (WT-1) and prostate apoptosis response gene-4 (*Par-4*), resulting in apoptosis/necrosis. These results suggest that targeting the fibroblast-to-myofibroblast transition with halofuginone may synergize with low doses of chemotherapy in achieving a significant antitumoral effect, avoiding the need of high-dose chemotherapy and its toxicity without impairing treatment efficacy. [Mol Cancer Ther 2007;6(2):570–7]

Introduction

Most solid tumors consist of a mixture of neoplastic and nonneoplastic cells together with extracellular matrix (ECM) components. This cellular microenvironment directly modulates tissue architecture, cell morphology, and cell fate (1, 2), and the ECM-stromal cell interaction contributes to the neoplastic phenotype (3). The conversion of fibroblasts into myofibroblasts, as mediated by transforming growth factor-β1 (TGF-β1), is the most prominent stromal reaction in a large number of epithelial lesions (4–6). In addition to the major increase in ECM components, the fibroblasts that acquire an activated phenotype, the myofibroblasts are characterized by expression of smooth muscle genes such as α-smooth muscle actin (*αSMA*) and *transgelin* (*SMA22α*; refs. 4, 7). The myofibroblasts are associated with the tumor cells at all stages of cancer progression (8) and, in various malignancies, tumor-dependent differentiation of fibroblasts toward myofibroblasts further promotes neoplastic progression (9–12).

It is well established that collagen type I, the major ECM component produced by myofibroblasts, not only functions as a scaffold for the tissue but also regulates the expression of genes associated with cellular signaling and metabolism, gene transcription, and translation, thus affecting fundamental cellular processes that are essential for tumor progression (13). Collagen type I accumulation has been observed at the tumor-stroma boundary (2, 14), and the TGF-β–dependent activation of neighboring stroma cells leads to a survival advantage and increased metastasis formation (15). Collagen type I has been hypothesized to be a signal for invasion, and its intratumoral expression level has been associated with increased tumor invasiveness (16, 17). The association of collagen type I with stellate cell activation–associated protein, also known as cytoglobin (Cygb/STAP), which has been hypothesized to regulate collagen synthesis under the control of TGF-β, is characteristic of cells that exhibit an activated phenotype (18, 19).

Cancer patients often face aggressive chemotherapy that involves multiple-treatment regimens, which are associated with significant side effects that adversely affect

Received 8/7/06; revised 11/26/06; accepted 12/12/06.

The costs of publication of this article were defrayed in part by the payment of page charges. This article must therefore be hereby marked *advertisement* in accordance with 18 U.S.C. Section 1734 solely to indicate this fact.

Note: Y. Sheffer and O. Leon contributed equally to this work.
This article is a contribution from the Agricultural Research Organization, Volcani Center, Bet Dagan, Israel.

Requests for reprints: Mark Pines, Institute of Animal Sciences, Volcani Center, P.O. Box 6, Bet Dagan, 50250, Israel. Phone: 972-8-9484408; Fax: 972-8-9475075. E-mail: pines@agri.huji.ac.il

doi:10.1158/1535-7163.MCT-06-0468

Published OnlineFirst January 31, 2007; DOI: 10.1158/1535-7163.MCT-06-0468

the patient's quality of life. Thus, an ideal anticancer treatment should simultaneously target both the malignant cells and their microenvironment to inhibit tumor growth, development, and invasion. Until recently, the lack of specific inhibitor(s) of any component of the ECM, in general, and of collagen type I, in particular, limited the success of such an approach. Halofuginone, an analogue of the plant alkaloid febrifugine, is an inhibitor of collagen type I synthesis (for review, see refs. 20, 21 and references therein). Halofuginone blocks TGF-β–mediated collagen synthesis by decreasing activation of Smad3 through increased expression of Smad7, an inhibitor of Smad2/3 activation, and by a c-jun–dependent mechanism (22–24). In culture, halofuginone attenuated collagen synthesis by skin fibroblasts from scleroderma and chronic graft-versus-host disease (cGvHD) patients. In animal models of fibrosis (adhesions, cGvHD, radiation-induced fibrosis, and pulmonary fibrosis), administration of halofuginone prevented the increase in collagen α1(I) gene expression and collagen synthesis. In the liver, halofuginone inhibited the synthesis of collagen type I and αSMA, resulting in inhibition of stellate cell activation and liver fibrosis (25). Human clinical efficacy was shown by topical dermal administration of halofuginone in patients with scleroderma and cGvHD (21). Halofuginone-dependent inhibition of collagen type I synthesis was associated with inhibition of microvessel formation *in vitro* and *in vivo* and resulted in decreased tumor growth in multiple murine models (26), including transplantable and chemically induced bladder carcinoma, glioma, von-Hippel-Lindau–associated pheochromocytoma (27), prostate cancer (28), and Wilms' tumor (29).

In the present study, we targeted the fibroblast-to-myofibroblast transition with halofuginone and evaluated its antitumoral effect alone or in combination with low dose of chemotherapy in human prostate and Wilms' tumor xenografts.

Materials and Methods

Materials

FCS, DMEM, and trypsin-EDTA solution (0.02–0.25%) were obtained from Biochemical Industries (Bet Haemek, Israel). Sirius red F3B was obtained from BDH Laboratory Supplies (Poole, United Kingdom). Halofuginone bromhydrate was obtained from Collgard Biopharmaceuticals Ltd. (Tel Aviv, Israel). Polyclonal rabbit anti-human prostate apoptosis response gene-4 (Par-4) and anti–Wilms' tumor suppressor gene product (WT-1) antibodies were obtained from Santa Cruz Biotechnology, Inc. (Santa Cruz, CA). Proliferating cell nuclear antigen staining kit was obtained from Zymed Laboratories (San Francisco, CA). Monoclonal antibodies to αSMA were from DAKO A/S (Glostrup, Denmark). Antibodies to Cygb/STAP were prepared as previously described (18). Dactinomycin (Cosmegen) was from Merck & Co., Inc. (West Point, PA); vincristine was from Pharmachemie BV (Haarlem, the Netherlands), and docetaxel (Taxotere) was from Aventis Pharma (Surrey, United Kingdom).

Animals and Experimental Design

All animal experiments were carried out according to the guidelines of the Volcani Center Institutional Committee for Care and Use of Laboratory Animals. Nude (CD1 *nu/nu*) male mice (Harlan Laboratories, Jerusalem, Israel) were housed in cages (four per cage) under conditions of constant photoperiod (12 light:12 dark) with free access to food and water. During the experiments, tumor size was determined with a caliper (formula: length × width × depth × 0.5236) and is presented as mean ± SE. Prostate cancer xenografts were established by implanting the human cell line PC3 (American Type Culture Collection, Rockville, MD) in Matrigel (4×10^6 cells/mL) s.c. using a 27-gauge needle (28). Treatments were initiated when the tumors reached a volume of 100 mm^3. Halofuginone was given in the diet at a concentration of 3 ppm throughout the experiment (~0.15–0.30 mg/kg). Docetaxel in saline (6 or 12.5 mg/kg) was administered i.v. into the tail vein on day 0 and 15 days later, and the control groups were treated with saline alone. The Wilms' tumor xenografts were established from tumors derived from a 3-year-old female with a stage I favorable histology tumor, in accordance with the National Wilms' Tumor Study Group. The establishment and maintenance of the Wilms' tumor xenografts were previously described in detail (29). Wilms' tumor cells (3×10^6) in Matrigel were injected s.c. and treatment was initiated 4 days later. Halofuginone (at 2 μg/mouse) was injected i.p. every other day. Chemotherapy was given as low doses of dactinomycin (0.525 mg/mL saline) once a week and of vincristine (0.583 mg/mL saline) once every 3 weeks, or as high doses of dactinomycin (1.575 mg/mL saline) once a week and of vincristine (1.75 mg/mL saline) once every 3 weeks.

Preparation of Sections, *In situ* Hybridization, and Immunohistochemistry

At the end of the experiments, tumors were collected and fixed overnight in 4% paraformaldehyde in PBS at 4°C. Serial 5-μm sections were prepared and embedded in Paraplast. Samples were stained with Sirius red for collagen. *In situ* hybridization for collagen α1(I) was done as previously described (25). The primers used for preparing the transgelin (SMA22α) probe were F-GGCCAACA-AGGGTCCATCCTAT and R-AGGACATTGGCTTCCAA-GGACA.

The sense probes elicited no signal. Immunohistochemistry was done with anti–Par-4 (1:500), anti–WT-1 (1:1,000), anti–Cygb/STAP (1:500), and anti-αSMA (1:200) antibodies. Peroxidase activity was revealed by using 3,3′-diaminobenzidine as chromogen.

Cell Culture and Northern Blots

The androgen-independent human prostate PC3 cancer cells were cultured in DMEM with 10% FCS in the presence of various concentrations of halofuginone. Total RNA was extracted with TRIzol reagent after 6 and 12 h, and *Par-4* gene expression was analyzed by Northern blotting. The primers used were F-GCAGATCGAGAA-GAGGAAGC and R-CATAAAAGGTGGCACACATCA, which resulted in a 998-bp probe.

Published OnlineFirst January 31, 2007; DOI: 10.1158/1535-7163.MCT-06-0468

Table 1. Effect of halofuginone, alone and in combination with docetaxel (Taxotere), on tumor development in prostate cancer xenografts

Treatment	Day 10	Day 21	Day 26	Day 30
	Volume $(mm)^3$			Weight (g)
Control	310 ± 60^a	450 ± 90^a	582 ± 111^a	1.56 ± 0.3^a
Halofuginone	126 ± 48^a	201 ± 97^{ab}	254 ± 95^{ab}	0.70 ± 0.2^{ab}
Taxotere (6 mg/kg)	247 ± 74^a	331 ± 97^{ab}	327 ± 89^{ab}	0.81 ± 0.2^{ab}
Halofuginone + Taxotere (6 mg/kg)	155 ± 51^a	173 ± 55^b	182 ± 63^b	0.46 ± 15^b
Taxotere (12.5 mg/kg)	226 ± 75^a	185 ± 50^b	186 ± 48^b	0.47 ± 10^b

NOTE: During the experiments, tumor volume was determined with caliper and tumor weight was evaluated at the end of the experiment. The results are presented as mean ± SE of five to seven animals in each group. In each column, means without a common superscript differ significantly ($P < 0.05$) according to Duncan's multiple range test.

Statistical Analysis and Image Analysis

Data were subjected to one-way ANOVA and means were separated by Duncan's multiple range test. Fibrosis levels, as exhibited by Sirius red staining, were analyzed by ImagePro software (Media Cybernetics, Inc. Silver Spring, MD). At least five sections taken from different animals were used and the mean results were expressed as arbitrary units.

Results

Effects of Combination Therapy on Tumor Development

Two animal models were used to evaluate the effect of inhibition of fibroblast activation by halofuginone, alone or in combination with low doses of chemotherapy, on tumor progression. In the control animals with prostate cancer xenograft, tumors derived from PC3 cells reached a mean volume of 582 mm^3 after 26 days and a mean weight of 1.56 g after 30 days. A trend in the reduction of tumor volume and weight was achieved with low doses of either halofuginone (3 ppm in the diet) or docetaxel (6 mg/kg) alone (Table 1). When the two treatments were combined, both the tumor volume and weight were significantly lower than those in the controls and reached the levels of tumors treated with a high dose of docetaxel (12.5 mg/kg). The same tendency was observed in the Wilms' tumor xenograft model: the control tumors reached a mean volume of 686 mm^3 84 days after tumor cell implantation (Table 2), and a low dose of halofuginone or of chemotherapy (dactinomycin and vincristine) caused a reduction in tumor volume at any point of evaluation. When the treatments were combined, a significant reduction in tumor volume as compared with that in the controls was observed, and it reached comparable measurements as in tumors treated with a high dose of chemotherapy. These results suggest that the combination of systemic treatment with a low dose of halofuginone, either given in the diet or injected i.p. together with a low dose of chemotherapy, results in the same therapeutic effect as high-dose chemotherapy alone.

Effect of Halofuginone on Fibroblast Activation

Acquisition of an activated phenotype by fibroblasts is associated with increased ECM production, especially of collagen type I and its regulator Cygb/STAP, and increased expression of the smooth muscle genes *αSMA* and *transgelin*. In both xenografts, the control, untreated tumors exhibited all the characteristics of activated fibroblasts [i.e., a large number of cells expressing the collagen (α1) type I gene resulting in high levels of collagen deposition (Fig. 1), as well as a large number of cells that synthesize Cygb/STAP and αSMA (Fig. 2)]. In addition,

Table 2. Effect of halofuginone, alone and in combination with chemotherapy, on tumor development in Wilms' tumor xenografts

Treatment	Day 66	Day 72	Day 75	Day 84
	Volume (mm^3)			
Control	71 ± 32^a	330 ± 50^a	338 ± 107^a	686 ± 100^a
Halofuginone	44 ± 31^a	80 ± 50^{ab}	84 ± 50^{ab}	125 ± 20^{ab}
Chemotherapy (low)	26 ± 12^a	56 ± 29^{ab}	67 ± 20^{ab}	99 ± 20^{ab}
Halofuginone + chemotherapy (low)	17 ± 3.0^a	24 ± 8.4^b	24 ± 8.5^b	30 ± 11^b
Chemotherapy (high)	11 ± 1.7^a	16 ± 2.3^b	18 ± 2.7^b	17 ± 2.6^b

NOTE: Chemotherapy was given at low doses of dactinomycin (0.525 mg/mL) once a week and vincristine (0.583 mg/mL) once every 3 wks or at high doses of dactinomycin (1.575 mg/mL) once a week and vincristine (1.75 mg/mL) once every 3 wks. During the experiments, tumor volume was determined with a caliper. The results are presented as mean ± SE of five to seven animals in each group. In each column, means without a common superscript differ significantly ($P < 0.05$) according to Duncan's multiple range test.

Published OnlineFirst January 31, 2007; DOI: 10.1158/1535-7163.MCT-06-0468

the activated fibroblasts in the Wilms' tumor xenografts expressed high levels of the *transgelin* (*SMA22α*) gene (Fig. 2). No transgelin expression was observed in the prostate cancer tumors of naïve or treated mice (data not shown). According to its unique mode of action, halofuginone inhibited the synthesis of all of these genes, both in the prostate cancer and in the Wilms' tumor xenografts, which suggests a similar mechanism of action. For example, collagen content (Sirius red staining) was inhibited with halofuginone alone by 2.3- and 2.0-fold and with αSMA by 2.5- and 1.7-fold in prostate cancer and Wilms' tumor xenografts, respectively. On the other hand, the expression of these genes and the synthesis of their proteins were not affected by the respective chemotherapies (docetaxel in prostate cancer, dactinomycin plus vincristine in Wilms' tumor xenografts). However, when the mice were treated with halofuginone and the respective chemotherapy, almost complete inhibition of synthesis of collagen (5.0- and 3.1-fold in prostate cancer and Wilms' tumor xenografts, respectively) and αSMA Cygb/STAP (4.1- and 3.5-fold in prostate cancer and Wilms' tumor xenografts, respectively) and of *transgelin* gene expression was observed (Table 3; Figs. 1 and 2).

Effect of Combination Therapy on WT-1 and Par-4

The *TGF-β1* gene is under the control of the Wilms' tumor suppressor gene product (WT-1) via the WT-1/Egr-1 consensus element in its promoter (30). The level of WT-1 was low in the untreated Wilms' tumor and prostate cancer xenografts (Fig. 3), but both halofuginone and the respective chemotherapy treatments caused major increases in WT-1 levels. In the prostate cancer tumors, an additive effect on WT-1 levels was observed when the mice were treated with both halofuginone and docetaxel whereas no such effect was observed in Wilms' tumor xenografts. However, in both xenografts, halofuginone and the respective chemotherapy caused reductions in tumor cell proliferation, which resulted in apoptosis/necrosis, as indicated by proliferating cell nuclear antigen staining. When the treatments were given together, only a small number of the tumor cells still maintained their cell cycle (Fig. 4). WT-1, through its zinc-finger DNA binding domain, interacts with the prostate apoptosis response gene-4 (Par-4) leucine repeat domain (31). Both halofuginone and docetaxel, alone and in combination, increased the level of Par-4 in PC3 xenografts by 9.2-, 9.5-, and 10.1-fold, respectively (Table 3; Fig. 4). In addition, halofuginone increased *Par-4* gene expression in PC3 cells in culture in a dose-dependent manner at all time points tested (Fig. 4). Par-4 was not detected in the Wilms' tumor xenografts before or after treatment either with halofuginone or with dactinomycin and vincristine, or with the two treatments in combination (data not shown).

Discussion

Increasing survival rates of cancer patients and the trend toward higher doses of toxic multimodality therapies have stimulated a focusing on the health-related quality of life of

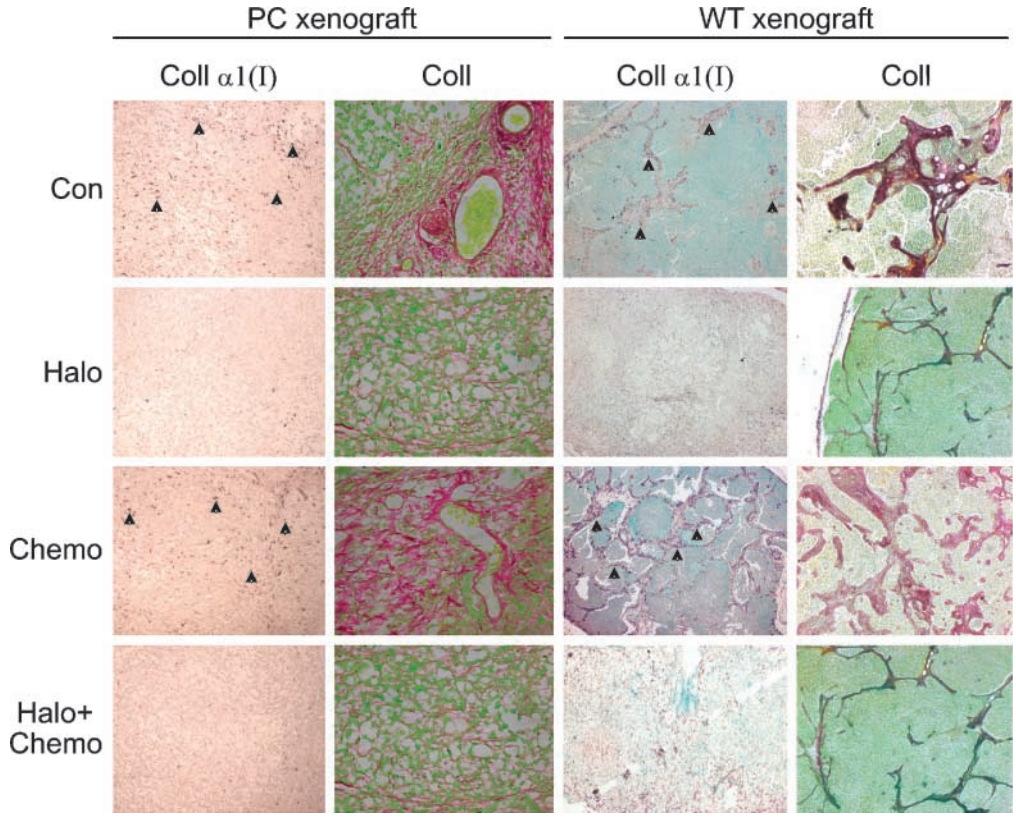

Figure 1. Collagen type I gene expression and collagen content in prostate cancer and Wilms' tumor xenografts. The untreated mice (*Con*) expressed a high level of collagen α1(I) gene (*arrows*) and a high level of collagen, as evaluated by *in situ* hybridization and Sirius red staining (collagen stained red), respectively. Halofuginone (*Halo*), alone or in combination with chemotherapy (*Halo* + *Chemo*), but not the respective chemotherapies alone (*Chemo*), attenuated collagen α1(I) gene expression and collagen content.

Published OnlineFirst January 31, 2007; DOI: 10.1158/1535-7163.MCT-06-0468

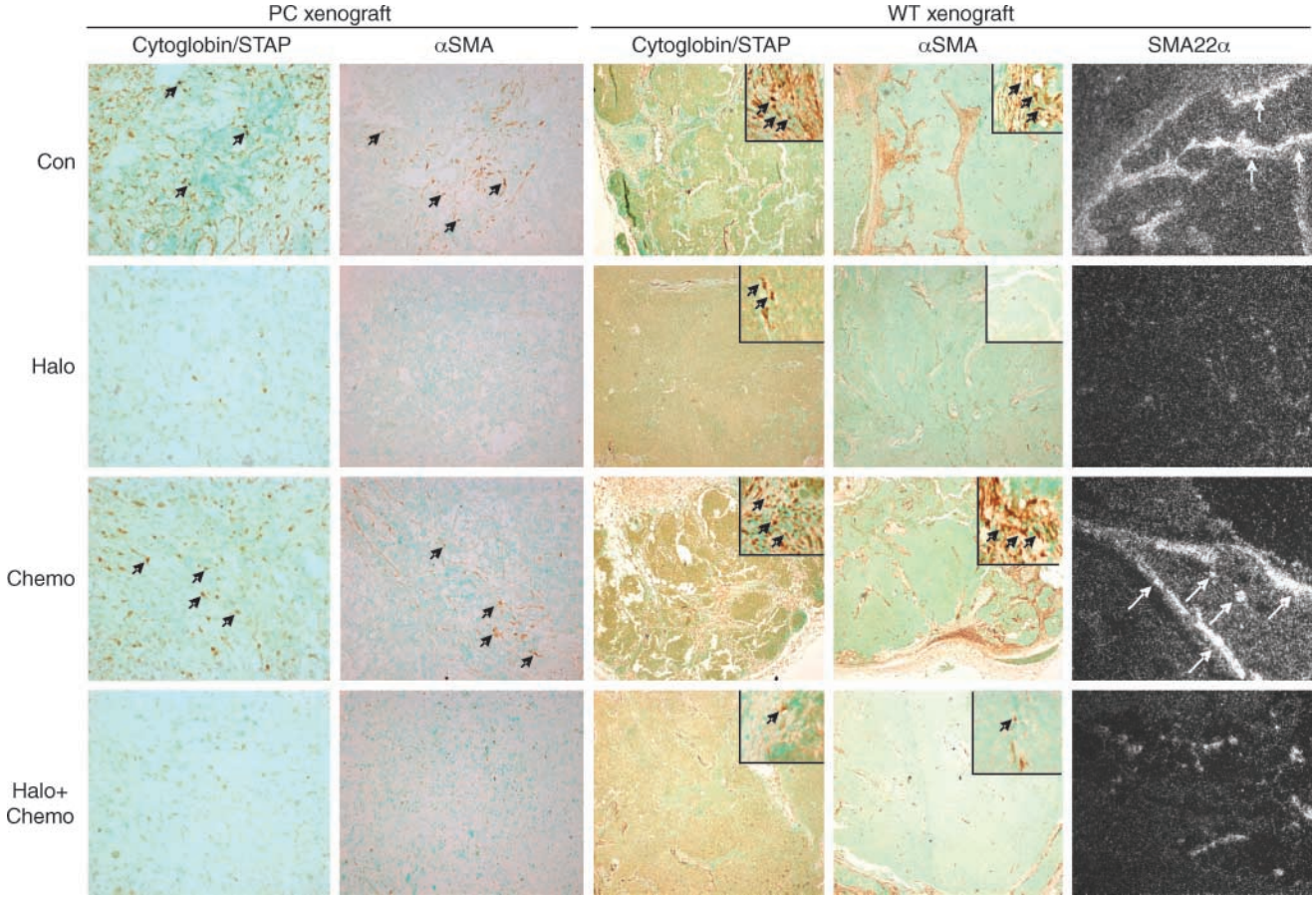

Figure 2. Cygb/STAP, αSMA, and transgelin in prostate cancer and Wilms' tumor xenografts. The untreated mice exhibit high levels of Cygb/STAP and αSMA (*arrows*), as evaluated by immunohistochemistry. Halofuginone, alone or in combination with chemotherapy, but not the respective chemotherapies alone, attenuated Cygb/STAP and αSMA levels. The untreated Wilms' tumor xenograft expressed high levels of the transgelin gene, as evaluated by *in situ* hybridization, which were inhibited by halofuginone, but not by dactinomycin and vincristine.

cancer survivors, which may continue to be of concern long after treatment has been discontinued. This applies especially in relation to Wilms' tumor pediatric patients, for whom the aim of most recent clinical trials has been to reduce the overall treatment burden, as the achievement of long-term survival by means of the heavy treatment burden is frequently accompanied by severe early and late complications (32). Myofibroblasts or cancer-associated fibroblasts together with ECM components provide the microenvironment that is pivotal for cancer cell growth, tumor invasion, and metastatic progression (8). Thus, inhibition of fibroblast activation may become a viable approach for tumor treatment, especially when combined with chemotherapy. In the prostate cancer and Wilms' tumor xenografts, low doses of halofuginone, independent of the route of administration, together with low doses of the respective chemotherapies, were as efficacious as the high chemotherapy doses (Tables 1 and 2). Thus, targeting the ECM and its cell population with halofuginone enables reduction in the chemotherapy dose without impairing the efficacy of the treatment. This is probably because diversity of modes of action is a prerequisite for a successful combination therapy. In prostate cancer and Wilms' tumor xenografts, halofuginone, but not the respective chemotherapies, affected collagen α1(I) gene expression and collagen content. These results are consistent with our previous findings that halofuginone inhibited collagen type I synthesis in various preclinical studies in which excess of collagen was the hallmark of the disease (20, 21), and halofuginone-dependent inhibition of collagen type I synthesis was correlated with reduction in tumor progression (26, 27). In addition, only halofuginone inhibited the synthesis of Cygb/STAP, which is known to regulate collagen synthesis under the control of TGF-β (18, 19), a finding that is consistent with the notion that halofuginone acts through the inhibition of Smad2/3 phosphorylation downstream of TGF-β (22–24). The expression of Cygb/STAP was up-regulated in fibrotic lesions of the pancreas and kidney in which activated fibroblast-like cells or myofibroblasts are known to proliferate (18). In the liver, Cygb/STAP is synthesized in activated stellate cells that are αSMA positive (33). Cygb/STAP probably is involved in

Published OnlineFirst January 31, 2007; DOI: 10.1158/1535-7163.MCT-06-0468

Table 3. Effect of halofuginone, alone and in combination with chemotherapy, on collagen, αSMA, Cygb/STAP, and Par-4 in prostate cancer and Wilms' tumor xenografts

Protein	Treatment			
	Control	Halofuginone	Chemotherapy	Halofuginone + chemotherapy
Collagen (arbitrary units)				
PC	0.85 ± 0.05[a]	0.37 ± 0.04[b]	0.80 ± 0.06[a]	0.17 ± 0.04[b]
WT	0.70 ± 0.05[a]	0.35 ± 0.05[b]	0.72 ± 0.04[a]	0.23 ± 0.03[b]
αSMA (arbitrary units)				
PC	0.61 ± 0.04[a]	0.24 ± 0.02[b]	0.65 ± 0.05[a]	0.15 ± 0.01[b]
WT	0.54 ± 0.08[a]	0.32 ± 0.04[b]	0.51 ± 0.04[a]	0.15 ± 0.03[b]
Cygb/STAP (arbitrary units)				
PC	0.92 ± 0.11[a]	0.45 ± 0.04[b]	0.89 ± 0.07[a]	0.23 ± 0.01[b]
WT	0.74 ± 0.11[a]	0.33 ± 0.08[b]	0.71 ± 0.08[a]	0.21 ± 0.01[b]
Par-4 (arbitrary units)				
PC	0.03 ± 0.01[a]	0.27 ± 0.06[b]	0.29 ± 0.04[b]	0.30 ± 0.04[b]

NOTE: Image analysis using ImagePro software was done on at least five sections taken from different animals and the mean results were expressed as arbitrary units. In each line, means without a common superscript differ significantly ($P < 0.05$) from the control according to Duncan's multiple range test.
Abbreviations: PC, prostate cancer; WT, Wilms' tumor.

cellular oxygen homeostasis and supply and plays a role as an O_2 reservoir that is used under hypoxic conditions, such as those occurring in fibrotic tissues and tumors with insufficient oxygen supply. Cygb/STAP expression is upregulated under hypoxia and is regulated by the hypoxia-inducible factor 1 (19), which regulates angiogenesis and is overexpressed in human cancers and their metastases (34). The inhibition of angiogenesis by halofuginone, in general (26), and of prostate cancer and Wilms' tumor xenografts, in particular (28, 29), may suggest the involvement, at least in part, of hypoxia-inducible factor 1–dependent Cygb/STAP overexpression in angiogenesis and tumor progression.

The fibroblast-myofibroblast transdifferentiation is associated with the expression of αSMA and transgelin (SMA22α). In hepatic fibrosis, halofuginone inhibited the activation of liver stellate cells, which is characterized by

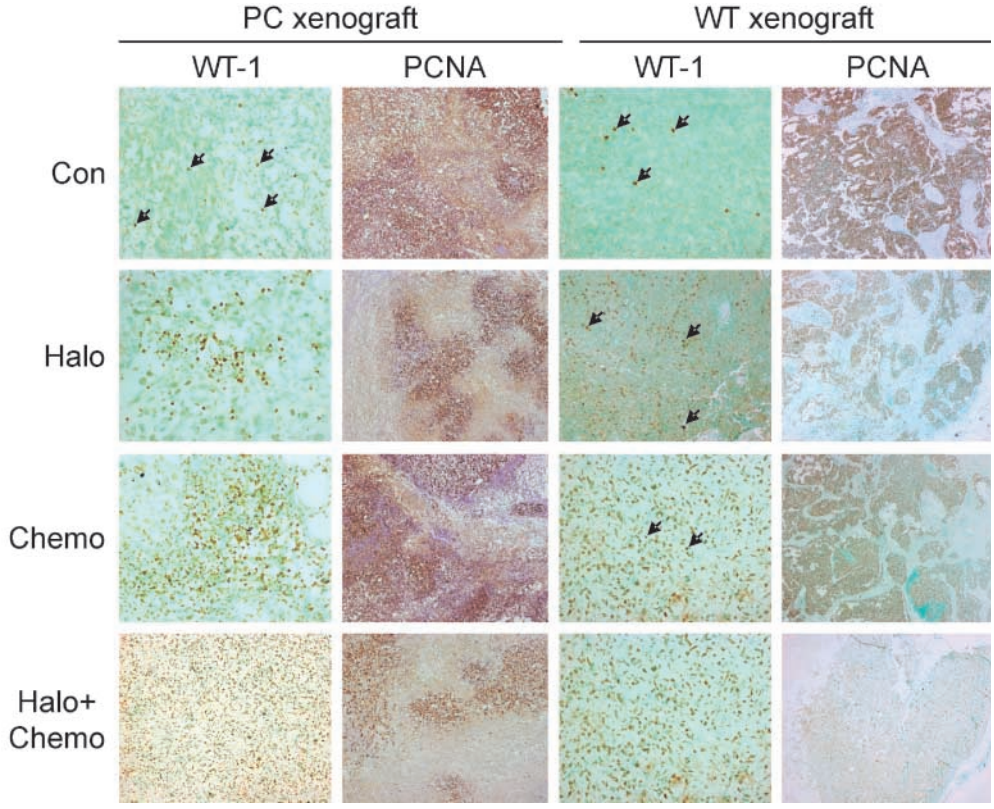

Figure 3. WT-1 and tumor cell cycle. A low level of WT-1 was observed in the untreated mice, as shown by immunohistochemistry (*arrows*). Both halofuginone and the respective chemotherapy caused increases in the level of WT-1. Most of the cells in the untreated mice are in their proliferative state, as indicated by immunohistochemistry with anti–proliferating cell nuclear antigen (*PCNA*) antibodies. Halofuginone and chemotherapy treatments caused apoptosis/necrosis, and when the mice were treated with both halofuginone and chemotherapy, almost no proliferative cells were observed.

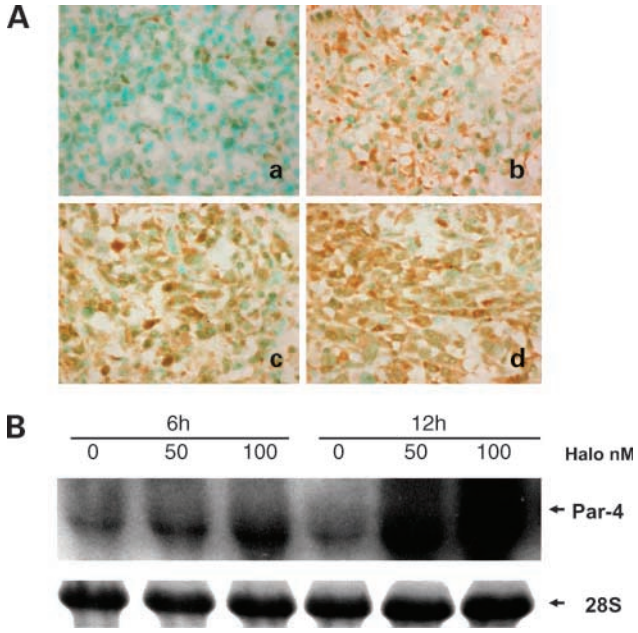

Figure 4. Par-4 in prostate cancer xenograft. **A,** immunohistochemistry of Par-4 in control mice (**a**), mice treated with halofuginone (**b**), mice treated with docetaxel (**c**), and mice treated with halofuginone in combination with docetaxel (**d**). **B,** PC3 cells were incubated with halofuginone and, at the end of the experiment, *Par-4* gene expression was detected by Northern blot analysis. The 28S rRNA was used as a control of RNA loading.

their transformation from quiescent, vitamin A–storing cells to highly proliferative, αSMA-positive cells that synthesize large amounts of collagen type I (25). The high levels of *transgelin* gene expression in the Wilms' tumor xenografts and the high levels of αSMA-positive fibroblasts in prostate cancer and Wilms' tumor control, untreated xenografts were inhibited by halofuginone, but not by the respective chemotherapies (Fig. 2). It is important to note that the αSMA-positive activated fibroblasts in the prostate cancer tumors did not express transgelin, and that even in the Wilms' tumor tumors, not all the αSMA-positive cells expressed transgelin, which suggests not only that the stromal fibroblasts differ from myofibroblasts of the reactive stroma but also that the myofibroblasts themselves are not a homogeneous population. This should be taken into account in strategic planning to inhibit the fibroblast-to-myofibroblast transition as a novel modality for cancer therapy. As transgelin and αSMA are regulated by TGF-β via the Smad3 pathway (35–37), halofuginone, an inhibitor of Smad3 phosphorylation, is probably an excellent candidate for such a strategy.

Previously, we showed that halofuginone stimulated the *in vitro* synthesis of the zinc-finger suppressor gene *WT-1* by Wilms' tumor and prostate cancer cells. In addition, halofuginone-dependent inhibition of Wilms' tumor growth was associated with increased synthesis of WT-1 (29). Overexpression of the *WT-1* gene has been observed in various tumors, although its specific role and those of its alternative splicing variants in tumorigenesis are not clear (38–40). In PC3 cells, halofuginone increased the level of the WT-1 54-kDa product but lowered that of the truncated 36-kDa product (data not shown). WT-1-induced apoptosis has been implicated in the actual development of the tumor (38, 41). In prostate cancer, WT-1 suppressed tumor cell growth, regulated the androgen-signaling pathway, and inhibited vascular endothelial growth factor expression, all of which are essential for tumor growth inhibition (42, 43). Although halofuginone induced a significant increase in WT-1 synthesis in both xenografts used, the respective chemotherapies induced WT-1 synthesis to a greater extent (Fig. 3). The halofuginone-dependent increase in WT-1 synthesis may be due to the interrelationships between WT-1 and TGF-β, which function via the WT-1/Egr-1 consensus element of the human TGF-β (30). The increases in WT-1 synthesis elicited by halofuginone and the respective chemotherapies were associated with a decrease in the number of proliferating cells and increased apoptosis/necrosis of tumor cells, especially when the treatments were applied in combination (Fig. 3). Thus, the beneficial effect of the combination therapy is probably greater than can be deduced from tumor size alone (Tables 1 and 2). The association of WT-1 and apoptosis in the prostate cancer xenograft was mediated, at least in part, by Par-4, one of the WT-1–interacting proteins that is functionally required, but is not sufficient, for apoptosis (31, 44). Halofuginone and the respective chemotherapies increased Par-4 in the prostate cancer xenograft and halofuginone increased *Par-4* gene expression in the PC3 cell line (Fig. 4).

At present, halofuginone is being evaluated in cancer clinical trials. Systemically, therapeutically effective plasma levels can be reached at a dosage that is well tolerated. No dose-limited toxicities were observed at 1 mg/d and the recommended dose for phase II studies of halofuginone is 0.5 mg administered daily (45). In cancer patients, the absorption of halofuginone after oral drug administration was associated with maximum peak drug levels at 3.4 ± 4.8 h. The estimated terminal elimination half-life had mean values of 28.3 ± 12.9 h, and only 4% to 12% of the administered dose of halofuginone was excreted unchanged in the urine, mainly in the first 24 h after drug administration. The area under the curve reached at the recommended dose of 0.5 mg/d is within the range in which antitumor efficacy was observed in preclinical studies (45). Consequently, thanks to the unique mode of action of halofuginone, its use in combination therapy, in association with other cancer-combating drugs that exhibit different modalities, is expected to successfully lower the dosages of chemotherapeutic drugs or to use less toxic compounds, thus offering reductions in the treatment burden imposed on cancer patients.

References

1. van Kempen LC, Rhee JS, Dehne K, Lee J, Edwards DR, Coussens LM. Epithelial carcinogenesis: dynamic interplay between neoplastic cells and their microenvironment. Differentiation 2002;70:610–23.

Published OnlineFirst January 31, 2007; DOI: 10.1158/1535-7163.MCT-06-0468

2. van Kempen LC, Ruiter DJ, van Muijen GN, Coussens LM. The tumor microenvironment: a critical determinant of neoplastic evolution. Eur J Cell Biol 2003;82:539 – 48.

3. Shekhar MPV, Pauley R, Heppner G. Host microenvironment in breast cancer development: extracellular matrix-stromal cell contribution to neoplastic phenotype of epithelial cells in the breast. Breast Cancer Res 2003;5:130 – 5.

4. Ronnov-Jessen L, Villadsen R, Edwards JC, Petersen OW. Differential expression of a chloride intracellular channel gene, CLIC4, in transforming growth factor-β1-mediated conversion of fibroblasts to myofibroblasts. Am J Pathol 2002;161:471 – 80.

5. Lewis MP, Lygoe KA, Nystrom ML, et al. Tumour-derived TGF-β1 modulates myofibroblast differentiation and promotes HGF/SF-dependent invasion of squamous carcinoma cells. Br J Cancer 2004;90:822 – 32.

6. Micke P, Ostman A. 2004 Tumour-stroma interaction: cancer-associated fibroblasts as novel targets in anti-cancer therapy? Lung Cancer 2004;45 Suppl 2:S163 – 75.

7. Untergasser G, Gander R, Lilg C, Lepperdinger G, Plas E, Berger P. Profiling molecular targets of TGF-β1 in prostate fibroblast-to-myofibroblast transdifferentiation. Mech Ageing Dev 2005;126:59 – 69.

8. Kalluri R, Zeisberg M. Fibroblasts in cancer. Nat Rev Cancer 2006;6: 392 – 401.

9. DeClerck YA. 2000 Interactions between tumour cells and stromal cells and proteolytic modification of the extracellular matrix by metalloproteinases in cancer. Eur J Cancer 2000;36:1258 – 68.

10. De Wever O, Mareel M. Role of myofibroblasts at the invasion front. Biol Chem 2002;383:55 – 67.

11. Tuxhorn JA, Ayala GE, Smith MJ, Smith VC, Dang TD, Rowley DR. Reactive stroma in human prostate cancer: induction of myofibroblast phenotype and extracellular matrix remodeling. Clin Cancer Res 2002;8: 2912 – 23.

12. Zidar N, Gale N, Kambic V, Fischinger J. Proliferation of myofibroblasts in the stroma of epithelial hyperplastic lesions and squamous carcinoma of the larynx. Oncology 2002;62:381 – 5.

13. Kiefer J, Alexander A, Farach-Carson MC. Type I collagen-mediated changes in gene expression and function of prostate cancer cells. Cancer Treat Res 2004;118:101 – 24.

14. van Kempen LC, Rijntjes J, Claes A, et al. Type I collagen synthesis parallels the conversion of keratinocytic intraepidermal neoplasia to cutaneous squamous cell carcinoma. J Pathol 2004;204:333 – 9.

15. Berking C, Takemoto R, Schaider H, et al. Transforming growth factor-β1 increases survival of human melanoma through stroma remodeling. Cancer Res 2001;61:8306 – 16.

16. van Hoorde L, van Aken E, Mareel M. Collagen type I: a substrate and a signal for invasion. Prog Mol Subcell Biol 2000;25:105 – 34.

17. Lockwood DS, Yeadon TM, Clouston AD, et al. Tumor progression in hepatocellular carcinoma: relationship with tumor stroma and parenchymal disease. J Gastroenterol Hepatol 2003;18:666 – 72.

18. Nakatani K, Okuyama H, Shimahara Y, et al. Cytoglobin/STAP, its unique localization in splanchnic fibroblast-like cells and function in organ fibrogenesis. Lab Invest 2004;84:91 – 101.

19. Schmidt M, Gerlach F, Avivi A, et al. Cytoglobin is a respiratory protein in connective tissue and neurons, which is up-regulated by hypoxia. J Biol Chem 2004;279:8063 – 9.

20. Pines M, Vlodavsky I, Nagler A. Halofuginone - a novel anti-fibrotic therapy. Gen Pharmacol 1997;30:445 – 50.

21. Pines M, Snyder D, Yarkoni S, Nagler A. Halofuginone to treat fibrosis in chronic graft versus host disease and scleroderma. Biol Blood Marrow Transplant 2003;9:417 – 25.

22. McGaha TL, Kodera T, Spiera H, Stan AC, Pines M, Bona CA. Halofuginone inhibition of COL1A2 promoter activity via a c-Jun-dependent mechanism. Arthritis Rheum 2002;46:2748 – 61.

23. McGaha TL, Phelps RG, Spiera H, Bona C. Halofuginone, an inhibitor of type-I collagen synthesis and skin sclerosis, blocks transforming-growth-factor-β-mediated Smad3 activation in fibroblasts. J Invest Dermatol 2002;118:461 – 70.

24. Xavier S, Piek E, Fujii M, et al. Amelioration of radiation-induced fibrosis: inhibition of transforming growth factor-β signaling by halofuginone. J Biol Chem 2004;279:15167 – 76.

25. Bruck R, Genina O, Aeed H, Alexiev R, Nagler A, Pines M. Halofuginone to prevent and treat thioacetamide-induced liver fibrosis in rats. Hepatology 2001;3:379 – 86.

26. Elkin M, Miao HQ, Nagler A, et al. Halofuginone: a potent inhibitor of critical steps in angiogenesis progression. FASEB J 2000;14:2477 – 85.

27. Pines M, Vlodavsky I, Nagler A. Halofuginone: from veterinary use to human therapy. Drug Dev Res 2000;50:371 – 8.

28. Gavish Z, Pinthus JH, Barak V, et al. Growth inhibition of prostate cancer xenografts by halofuginone. Prostate 2002;51:73 – 83.

29. Pinthus JH, Sheffer Y, Nagler A, Mor Y, Genina O, Pines M. Inhibition of Wilm's tumor xenografts progression by halofuginone is accompanied by activation of WT1 gene expression. J Urol 2005;174: 1527 – 31.

30. Dey BR, Sukhatmem VP, Roberts AB, et al. Repression of the transforming growth factor-β1 gene by the Wilms' tumor suppressor WT1 gene product. Mol Endocrinol 1994;8:595 – 602.

31. Sells SF, Han SS, Muthukkumar S, et al. 1997 Expression and function of the leucine zipper protein Par-4 in apoptosis. Mol Cell Biol 1997;17:3823 – 32.

32. Kalapurakal JA, Dome JS, Perlman EJ, et al. Management of Wilms' tumour: current practice and future goals. Lancet Oncol 2004;5:37 – 46.

33. Kawada N, Kristensen DB, Asahina K, et al. Characterization of a stellate cell activation-associated protein (STAP) with peroxidase activity found in rat hepatic stellate cells. J Biol Chem 2001;276: 25318 – 23.

34. Hirota K, Semenza GL. Regulation of angiogenesis by hypoxia-inducible factor 1. Crit Rev Oncol Hematol 2006;59:15 – 26.

35. Ronnov-Jessen L, Petersen OW. Induction of α-smooth muscle actin by transforming growth factor-β1 in quiescent human breast gland fibroblasts. Implications for myofibroblast generation in breast neoplasia. Lab Invest 1993;68:696 – 707.

36. Hu B, Wu Z, Phan SH. Smad3 mediates transforming growth factor-β-induced α-smooth muscle actin expression. Am J Respir Cell Mol Biol 2003;29:397 – 404.

37. Qiu P, Ritchie RP, Fu Z, et al. Myocardin enhances Smad3-mediated transforming growth factor-β1 signaling in a CArG box-independent manner: Smad-binding element is an important cis element for SM22α transcription *in vivo*. Circ Res 2005;97:983 – 91.

38. Lee SB, Haber DA. Wilms tumor and the WT1 gene. Exp Cell Res 2001;264:74 – 99.

39. Loeb DM, Sukumar S. The role of WT1 in oncogenesis: tumor suppressor or oncogene. Int J Hematol 2002;76:117 – 26.

40. Tuna M, Chavez-Reyes A, Tari AM. HER2/neu increases the expression of Wilms' Tumor 1 (WT1) protein to stimulate S-phase proliferation and inhibit apoptosis in breast cancer cells. Oncogene 2005;24:1648 – 52.

41. Morrison DJ, English MA, Licht JD. WT1 induces apoptosis through transcriptional regulation of the proapoptotic Bcl-2 family member Bak. Cancer Res 2005;65:8174 – 82.

42. Graham K, Li W, Williams BR, Fraizer G. Vascular endothelial growth factor (VEGF) is suppressed in WT1-transfected LNCaP cells. Gene Expr 2006;13:1 – 14.

43. Fraizer G, Leahy R, Priyadarshini S, Graham K, Delacerda J, Diaz M. 2004 Suppression of prostate tumor cell growth *in vivo* by WT1, the Wilms' tumor suppressor gene. Int J Oncol 2004;24:461 – 71.

44. Richard DJ, Schumacher V, Royer-Pokora B, Roberts SG. 2001 Par-4 is a coactivator for a splice isoform-specific transcriptional activation domain in WT1. Genes Dev 2001;15:328 – 39.

45. de Jonge MJA, Dumez H, Verweij J, Yarkoni S, et al. Phase I and pharmacokinetic study of halofuginone, an oral quinazolinone derivative in patients with advanced solid tumours. Eur J Cancer 2006;42: 1768 – 74.

AACR American Association for Cancer Research

Molecular Cancer Therapeutics

Inhibition of fibroblast to myofibroblast transition by halofuginone contributes to the chemotherapy-mediated antitumoral effect

Yuval Sheffer, Oded Leon, Jehonathan H. Pinthus, et al.

Mol Cancer Ther 2007;6:570-577. Published OnlineFirst January 31, 2007.